Identification of parameters of Maxwell and Kelvin-Voigt generalized models for fluid viscous dampers

Identification of parameters of Maxwell and Kelvin-Voigt generalized models for fluid viscous dampers

RITA GRECO

DICATECH, Technical University of Bari, via Orabona 4 - 70125, Bari -Italy.

GIUSEPPE C MARANO[2]

DICAR, Technical University of Bari, via Orabona 4 - 70125, Bari -Italy.

Corresponding author:

Giuseppe Carlo Marano DICAR, Technical University of Bari, via Orabona 4 - 70125, Bari -Italy, Email: g.marano@poliba.it.

Abstract

Fluid Viscous Dampers have been widely applied to reduce the effects of vibrations in civil engineering structures. Good understanding of the dynamical behavior of these devices is required for the analysis of structures equipped with Fluid Viscous Dampers. The simple Kelvin–Voigt and Maxwell rheological models do not have enough parameters to suitably capture the frequency dependence of device parameters and for this purpose other models representing some generalizations of basic Kelvin–Voigt and Maxwell models have been developed. This paper is devoted to parameters identification basic and generalized Kelvin–Voigt and Maxwell models for Fluid Viscous Dampers. The identification procedure furnishes the best mechanical parameters by minimizing a suitable objective function that represents a measure of difference between analytical and experimental applied forces. For this purpose the Particle Swarm Optimization is adopted. Results are obtained under various test conditions, comparing the agreement of various models with experimental data. Finally, a numerical investigation is performed on a simple one degree of freedom structure, equipped with Fluid Viscous Dampers and subject to a real seismic motion.

Keywords

Vibration control, fluid viscous damper, Kevin-Voigt model, Maxwell model, parameters identification, particle swarm optimization.

1. Introduction

Among various passive vibration control technologies adopted to reduce detrimental effects associated to large vibrations in civil structures (Marano et al., 2010, and Marano et al, 2007) additional damping represents one of the different ways that have been projected over the year to allow structures to achieve optimal performances when they are subjected to external actions. Conventional approach would dictate that the structure must inherently attenuate or dissipate the effects of transient inputs through a combination of strength, flexibility and deformability. However, generally, the level of damping in a conventional elastic structural system is very low, and therefore the amount of energy dissipated during transient excitations is also very low. For example, during strong earthquakes conventional structures typically deform well beyond their elastic limits, and eventually fail or collapse. Therefore, most of the energy dissipated is absorbed by the structure itself which is subjected to damage. Adding supplemental dampers to a structure has, as consequence, that much of the energy introduced into the structure will be absorbed, not by the structure but by the additional devices properly designed for this purpose.

Additional damping can be provided by fluid and solid viscous dampers. Silicone oil is used to build the fluid dampers, while the solid dampers are made of copolymers or glassy substances. The Fluid Viscous devices developed in recent times include Viscous Walls and Fluid Viscous Dampers (FVD) which represent the object of this study. The Viscous Wall, developed by Sumitomo Construction Company, consists of a plate moving in a thin steel case filled with highly viscous fluid (Soong and Spencer, 2002).

FVD operates on the principle of fluid flow through orifices. A stainless steel piston travels through chambers that are filled with silicone oil. The silicone oil is inert, non flammable, non toxic and stable. The pressure difference between the two chambers produces silicone oil to flow through an orifice in the piston head: input energy is then transformed into heat, which dissipates into the atmosphere. The force/velocity law can be characterized as $F = C\dot{x}^{\alpha}$ where F is the output force, $\dot{x}$ the relative velocity across the damper, C is the damping coefficient and α is a constant which assumes usually a value between 0,3 and 1,0.

In order to enhance the effectiveness of application of FVD and in order to provide a reliable support for designing an efficient protection strategy, a suitable description of behavior of these dampers is needed. In the past different models were developed to describe the dynamic behavior of viscous dampers and both the classical and the so-called fractional-derivative models of viscous dampers are available. The simple models, like the Maxwell model and the Kelvin-Voigt model (Zhao-Dong, 2007; Zhao-Dong et al., 2011; Sing et al., 2003; Lee et al., 2004) are very frequently adopted to represent FVD. For example the Kelvin–Voigt model, which consists of the spring and the dashpot connected in parallel, is used in papers (Singh and Moreschi, 2002; Shukla and Datta, 1999; Galucvio et al., 2004), while the Maxwell model built from the serially connected spring and dashpot is used in (Lee et al. 2004; Hatada et al., 2000;Sing and Moreschi, 2002; Shukla and Datta, 1999).

However, these models present the disadvantage to correctly model the mechanical properties of the dampers only for individual frequencies. On the contrary, the mechanical properties of the polymers used in these devices are strongly frequency dependent and for this purpose standard mechanical rheological models, whose parameters are determined from experimental studies, like the generalized Maxwell or generalized Kelvin - Voigt models, have been often used the FVD (Park, 2001; Park, 2001).

Fractional models are becoming more and more popular because of their ability to describe the behavior of visco-elastic dampers using a small number of parameters. Using the fractional calculus a number of rheological models, e.g., the fractional Kelvin– Voigt model (Papoulia et al., 2010), the fractional Zener model (Pritz, 1996; Atanackovic, 2002), the fractional Jeffreys model (Soong and Jiang, 1998), the fractional Maxwell model (Makris and Constantinou, 1991) and the fractional derivative Maxwell Model (Jiu et al., 2007) have been proposed. It has been shown in (Park, 2001) and (Schmidt and Gaul, 2002) that the fractional derivative models can better capture the frequency dependent properties of viscous dampers. However, a significant problem related with the fractional rheological models, is the evaluation of model parameters from experimental data. Various methods have been utilized to evaluate model parameters from both static and dynamic tests (Gerlach and Matzenmiller, 2005; Syed and Philips, 2000; Aprile et al., 1997; Hansen, 2007; Gaul and Schmidt, 2002). The process of parameter identification is an inverse problem which is over determined and can be ill conditioned (see, for example (Syed and Philips, 2000; Hansen, 2007) because of noises existing in the experimental data. The mathematical difficulties may be surmounted by the regularization method which is described, for example, in (Gerlach and Matzenmiller, 2005).

Current identification techniques for viscous dampers are mostly based on parametric models. Although parametric identification techniques have been successfully used to identify viscous dampers, non-parametric identification techniques are more suitable in structural health monitoring SHM (Soong and Dargush, 1998) because the system characteristics may continuously vary over time, both quantitatively as well as qualitatively. Several identification approaches, both parametric and nonparametric, are compared in (Yun and Bahng, 2000; Yun et al., 2008) by using real data carried out from full-scale nonlinear viscous dampers commonly used with large flexible bridges. About the parametric techniques, the capability of the Adaptive Random Search is explored in (Yun and Bahng, 2000): the authors solved an optimization problem in which the numerical values of the unknown model parameters were estimated by minimizing an objective function based on the

normalized mean square error between the measured and identified damper responses, evaluated as displacement/velocity and obtained by integrating dynamic equilibrium equations of FVD constitutive law subject to experimental applied force history.

This paper focuses on the evaluation of performance of classical and generalized Kelvin-Voigt and Maxwell models for FVD modeling. In the study here proposed generalized Kelvin-Voigt (GKV) model and Generalized Maxwell model (GMM) are a modification of the classical Kelvin-Voigt and Maxwell models, where the main difference between classical and generalized models is that the generalized one incorporates nonlinearity in both the spring and the viscous element. More precisely, the resistant forces of both elements in these two generalized models have fractional exponential coefficients. In order to assess the efficiency of these generalized models to capture the hysteretic behavior of real FVD, analytical models will be verified by experimental test. Therefore, the identification scheme is developed comparing the experimental and the analytical values of the forces experienced by the device under investigation, where the experimental one has been recorded during the dynamic test, while the analytical one is obtained by applying a displacement time history to the candidate mechanical law. In this way, a measure of the "distance" between experimental and analytical result is introduced as the integral of the difference along the whole experiment considered. The optimal set of parameters is thus derived by minimizing this distance by using an evolutionary algorithm. For the parametric identification of a real FVD the authors adopt the Particle Swarm Optimization (PSO). Identification is carried out under various test conditions comparing also generalized and standard models: some considerations about agreement with experimental data are also furnished. Finally, a numerical investigation is performed on a simple one degree of freedom structure equipped with a FVD and subject to a real seismic motion. For FVD classical and generalized models are considered whose parameters have been previously identified.

The next of the paper is organized as follows: in section 2 a survey of standard and generalized Kelvin-Voigt and Maxwell models is reported. In section 3 the identification scheme is reassumed and some remarks of PSO algorithm are given. Moreover, in section 4 some details of experimental test are furnished and in section 5 the results of the identification are illustrated and some conclusions are carried out. In section 6 a numerical investigation on a simple one degree of freedom structural system equipped with FVD and subject to a real seismic motion is performed in order to assess the variability of the response to device modeling. In section 7 come conclusions are then discussed.

2. Mechanical models for fluid viscous dampers

In this paper two rheological models, i.e. the Kelvin-Voigt and the Maxwell models (see Figure 1), are used to describe the dynamic behavior of FVD. This selection has been made because, due to their simplicity, Kelvin–Voigt and Maxwell models are adopted frequently to represent the behavior of viscous dampers.

2.1 Kelvin-Voigt model

Experimental studies have demonstrated that the resistance force of some viscous dampers depends not only on damper velocity but also on damper deformation. This mechanical property may be mathematically modeled connecting a spring element and a viscous element, respectively. In the Kelvin–Voigt model these two elements are connected in parallel (Figure 1a). The equation of the motion of this element can be written as

$$F = Kx + C\dot{x} \tag{1}$$

In equation (1) F represents the damper (axial) force; x denotes the damper deformation, $\dot{x}$ represents the deformation rates; K denotes the stiffness value of the spring element; C is the damping coefficient of the viscous element.

This classical model can be generalized incorporating a nonlinearity in both the spring and the viscous element (Figure 1b); the resistant forces of both elements in this generalized model have fractional exponential coefficients

$$F = Kx^{\beta} + C\dot{x}^{\alpha} \tag{2}$$

In this study the classical and generalized Kelvin-Voigt models given in equations (1) and (2) will be employed to simulate a nonlinear FVD. For these models two characteristic parameters, K and C (classical Kelvin-Voigt model) or four characteristic parameters, K, C, α and β (generalized Kelvin-Voigt model) must be identified.

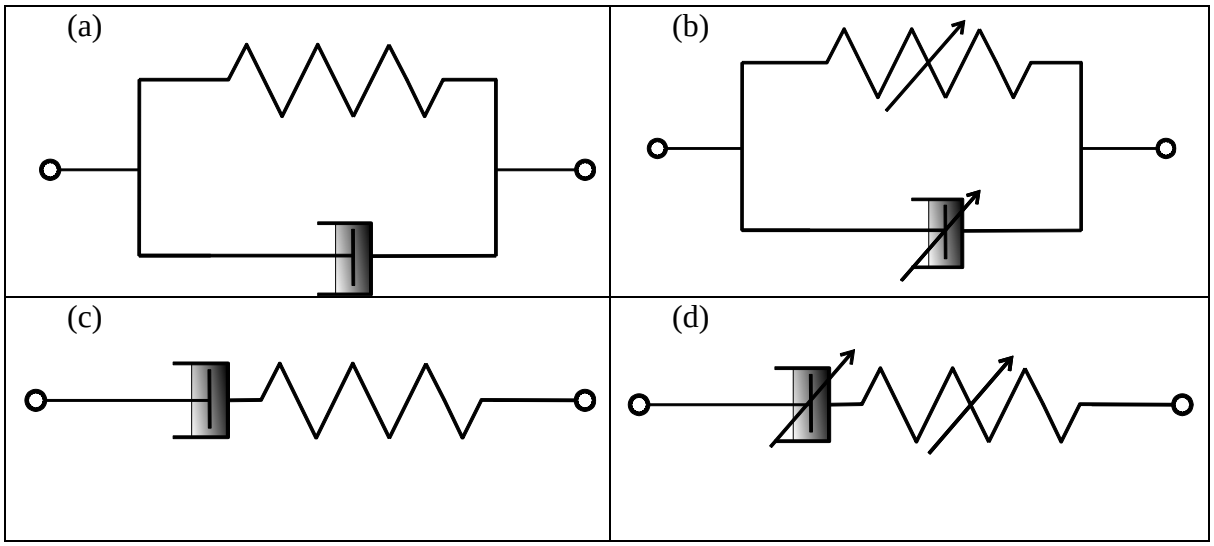

Figure 1. Rheological models of viscous damper: (a) Kelvin-Voigt, (b) Generalized Kelvin-Voigt, (c) Maxwell, (d) Generalized Maxwell.

2.2 Maxwell model

In the Maxwell model the spring and the dashpot element are connected in series (Figure 1c). Mechanically this model must satisfy the following kinematic conditions

$$x = x_e + x_v$$

$$\dot{x} = \dot{x}_e + \dot{x}_v \tag{3}$$

and also the following force condition

$$F = Kx_e = C\dot{x}_v \tag{4}$$

In equation (4) F represents the damper (axial) force; x denotes the total damper deformation; x_e and x_v denote the deformations of the stiffness and viscous components, respectively. In addition $\dot{x}$, $\dot{x}_e$ and $\dot{x}_v$ represent the corresponding to x, x_e and x_v; K denotes the stiffness value of the spring element; C is the damping coefficient of the viscous element.

Also this classical model can be generalized incorporating a nonlinearity in both the spring and the viscous element (Figure 1d); the resistant forces of both elements in this generalized model have fractional exponential coefficients

$$F = Kx^{\beta}{}_e = C\dot{x}_v^{\alpha} \tag{5}$$

In this study also the classical and generalized Maxwell models given in Eq. (4) and (5) will be employed to simulate a nonlinear FVD. For these models the two characteristic parameters, *K* and *C* (classical Maxwell model) or the four characteristic parameters, K, C, α and β (generalized Maxwell model) must be determined.

2.3 Numerical method for the Generalized Maxwell model

In this section it will briefly develop the numerical method used in the simulation of the generalized Maxwell model, needed in the next part of this paper to simulate the model response to compare with experimental data. Because the hysteresis loop of a damper is the relation between the damper force *F* and the total damper deformation *x*, first of all one needs to solve *F* as a function of *x*.

For this purpose equation (5) can be written as

$$\dot{x}_v = \left(\frac{K}{C}\right)^{\frac{1}{\alpha}} x_e^{\frac{\beta}{\alpha}} \tag{6}$$

In addition from equation (3) it results

$$\dot{x}_e = \dot{x} - \dot{x}_v \tag{7}$$

and then

$$\dot{x}_e = -\left(\frac{K}{C}\right)^{\frac{1}{\alpha}} x_e^{\frac{\beta}{\alpha}} + \dot{x} \tag{8}$$

Now, if the damper total deformation x is assigned and is considered as an external excitation, equation (8) represents the dynamic equation of the generalized Maxwell model forced by prescribed disturbance $\dot{x}$. Mathematically this equation is also a first-order ordinary differential equation with $\dot{x}_e$ and it can be solved by many numerical methods. Once the differential equation has been solved in $\dot{x}_e$ one can obtain F.

3. Identification scheme: objective function and optimization problem

Identification aims to evaluate the four parameters K, C, α and β (generalized models) or only the two parameters K, C (classical models). These are collected in the vector $\overline{\Theta}$, named parameter vector, that is a two or four dimensions vector, respectively, in case of classical or generalized models. After the design vector has been specified, the second step for parameters identification scheme requires the formalization of a suitable objective function to be minimized.

The model parameters $\mathbf{x}$ of the viscous damper are identified by solving the following single-objective optimization problem

$$\min_{\mathbf{x}} \left\{ f(\mathbf{x}) \right\} \tag{9}$$

$$\text{s.t. } \mathbf{x}^l \le \mathbf{x} \le \mathbf{x}^u$$

in which $\mathbf{x} = \{x_1,\ldots,x_j,\ldots,x_n\}$ is a set of real parameters, in this case $\mathbf{x}$ collects the mechanical models parameters, $\mathbf{x}^l = \{x_1^l,\ldots,x_j^l,\ldots,x_n^l\}$ and $\mathbf{x}^u = \{x_1^u,\ldots,x_j^u,\ldots,x_n^u\}$ are its lower and upper bounds, respectively. The solution that minimizes the objective function $f(\mathbf{x})$ (OF) is denoted as $\mathbf{x}^*$.

The following integral is assumed as a suitable measure to define the OF in the identification problem:

$$OF(\mathbf{x}) = \frac{\int_{t_{start}}^{t_{end}} abs\left(f_{\exp}(t) - f_e(\mathbf{x},t)\right)dt}{\int_{t_{start}}^{t_{end}} abs\left(f_{\exp}(t)\right)dt} \tag{10}$$

where t_{start} and t_{end} are the start and end time records, $f_{exp}(t)$ is the experimental force measured, while $f_e(t)$ is the force estimated obtained by numerical differentiation of experimental displacement time history with a 3rd order algorithm to limit numerical noise.

The OF evaluation is extremely computational cheap if compared to the alternative dissimilar approaches, in which the duality of starting from an experimental force leads to the theoretical displacement obtained by integration as a solution of the differential equation. In order to solve the problem previous stated Particle Swarm Optimization (PSO) is adopted. PSO is a population-based stochastic optimization technique appropriate for global optimization with no need for direct evaluation of gradients. Introduced by Kennedy and Eberhart (1995), the method mimics the social behavior of flocks of birds and swarms of insects and assures the axioms of swarm intelligence, namely proximity, quality, diverse response, stability and adaptability. The basic PSO algorithm variant works by having a population of possible solutions that are moved around in the research space according to a few simple formulae. Their movements are guided by their own best known position in the search-space as well as the entire swarm's best known position. In some more details there are two primary operators; position update and velocity update. Each particle during each

generation is accelerated toward the particles previous best position and the global best position. The evaluation of new velocity in each iteration for each particle is referred to its current velocity, the distance from its previous best position, and the distance from the global best position. When improved positions are being discovered these will then come to guide the movements of the swarm. The process is repeated and by doing so it is hoped, but not guaranteed, that a satisfactory solution will eventually be discovered.

4. Experimental studies

4.1 Test device

The 750 kN viscous damper was tested at SISMALB laboratory in Taranto, Italy. The test setup (Figure 2) consists of a high resistance steel frame to withstand loads of tension and compression of 2200 kN. The device is anchored to structure by means of a pin, and is stilled to the servant cylinder by means of a threaded connection and bolted. The movements are generated by a servant cylinder of 1400 kN, controlled in force and/or displacement. Between servant cylinder and device is located a load cell of 2500 kN, which acquires the forces applied to the device during the entire duration of the experiment. In a displacement imposed test, the device movements are controlled by a transducer mounted on the device. The control and data acquisition system is able to generate a real time analysis device displacements by instantaneous variation of applied forces by the servant cylinder, by means of a computer automatic control hydraulic pressure system. The displacement time history should be imposed with different laws, from sinusoidal to triangular, or through a generator step of generic ones. Acquiring systems have 30 channels and can command 2 actuators at the same time. Table 1 shows the design characteristics of the tested FVD. The imposed time displacement history adopted is a sinusoidal one with a transient initial phase to reach the stationary regime; the same is at the end of the process, when a decreasing phase is adopted. In both the

phases (starting and ending) the automatic control system use a variable amplitude process whit the same frequency of the stationary one. Amplitude increase with a linear low so that in two pulsations it reaches the final value. Some noise due in control phase are in those two phases, especially in first 2 – 3 seconds, and are related to the difficulty in controlling instantaneously this process from the beginning, but it do not decrease sensibly test accuracy.

(a)

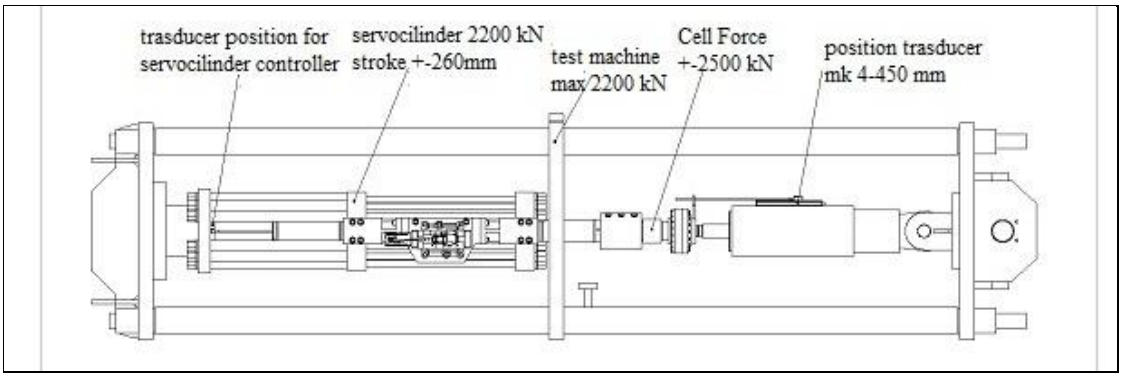

(b)

Figure 2. (a) A photo of the test apparatus with the FVD and (b) a schematic description .

F [kN]	Stroke [mm]	C [kN/(mm/s)]	V [mm/s]	α
750	± 100	406.24	460	0.1

Table 1. FVD Design Condition.

4.2 Test cases

Three experiments were performed to obtain dynamic response of the viscous damper. The experiments were designed to determine the dynamic performance characteristics of the damper at varying velocities and to determine the effective energy dissipation of the device. The damper was subjected to multiple sets of monotonic sinusoidal excitations at peak velocities of 92 *mm/s* and 460 *mm/s*. The first two tests had a 3-cycle excitation period, while the third test (energy dissipation test) had a 10-cycle period. The specifications of test are summarized in Table 2.

No.	Load (kN)	Test stroke (±mm)	Velocity (mm/s)	Cycles
Test 1	750	20	92	3
Test 2	750	20	460	10
Test 3	750	20	460	3

Table 2. Fluid viscous damper test condition.

5. Parameters identification results

For the evaluation of optimal values of the unknown quantities the parametric identification which makes use of a non-classical method (PSOA) was applied with a population size N=50 and

maximum number of iterations L=100. The parametric identification has been performed by solving the single-objective optimization problem whose objective function is given by Equation (10). The algorithms have been performed fifty times and the best solution has been carried out as the final identification result. These are shown in table 3 for each test and for each model examined.

Voigt					
	C		*K*		*OF*
Test 1	*6.4963*		*12.6587*		*0.2877*
Test 2	*3.5944*		*15.5999*		*0.2049*
Test 3	*3.0240*		*12.8350*		*0.3074*
Maxwell					
	C		*K*		*OF*
Test 1	*7.3107*		*139.2401*		*0.2882*
Test 2	*4.0123*		*259.4377*		*0.1784*
Test 3	*3.3335*		*205.6275*		*0.2869*
Generalized Voigt					
	C	*K*	α_c	β_k	*OF*
Test 1	*24.1856*	*0.7847*	*0.6932*	*2.0000*	*0.2300*
Test 2	*1.0213*	*1.1889*	*1.2407*	*2.0000*	*0.1816*
Test 3	*4.7018*	*52.2115*	*0.9249*	*0.4756*	*0.3079*
Generalized Maxwell					
	C	*K*	α_c	β_k	*OF*
Test 1	*132.0147*	*267.8712*	*0.3331*	*1.0006*	*0.1269*
Test 2	*122.1587*	*358.5821*	*0.3360*	*1.0060*	*0.1240*
Test 3	*119.2544*	*277.8710*	*0.3333*	*1.0017*	*0.1535*

Table 3. Identified parameters for the four analyzed models for FVD.

More precisely, for each model the minimized objective function is furnished together with optimum parameters obtained by solving the optimization problem given in equation (9),. i.e. the parameters that best fit the experimental cycles of FVD, and this is achieved by using the optimization searching scheme PSO. The results are distinguished for different tests in order to assess the influence on the solution performance of the frequency, of the load application and of the cycles number.

In Figures 3-6 the experimental hysteresis loops of the damper are compared with those simulated by the selected models previous described, for load application velocities V_1, V_2 (in figures different tests are individuated with $Test_1$ $Test_2$ and $Test_3$. More precisely, in Figures 3-6 both relationships force-displacement (a) and force-velocity (b) are shown. The blue lines represent the experimental loops, while the red lines are the theoretical loops obtained by using the identified parameters for each model.

By observing the plots one can notice that the experimental and theoretical loops have exactly the same relative displacement (and velocity), whereas the damper force of the theoretical loop is computed according to each of the models. The comparison between theoretical and simulated loops points out that the analyzed models have a different ability to capture the hysteretic behavior of the fluid damper under excitations of different frequencies and different number of cycles; this last aspect is related to the relative importance of the transient response with respect to the entire duration of the load.

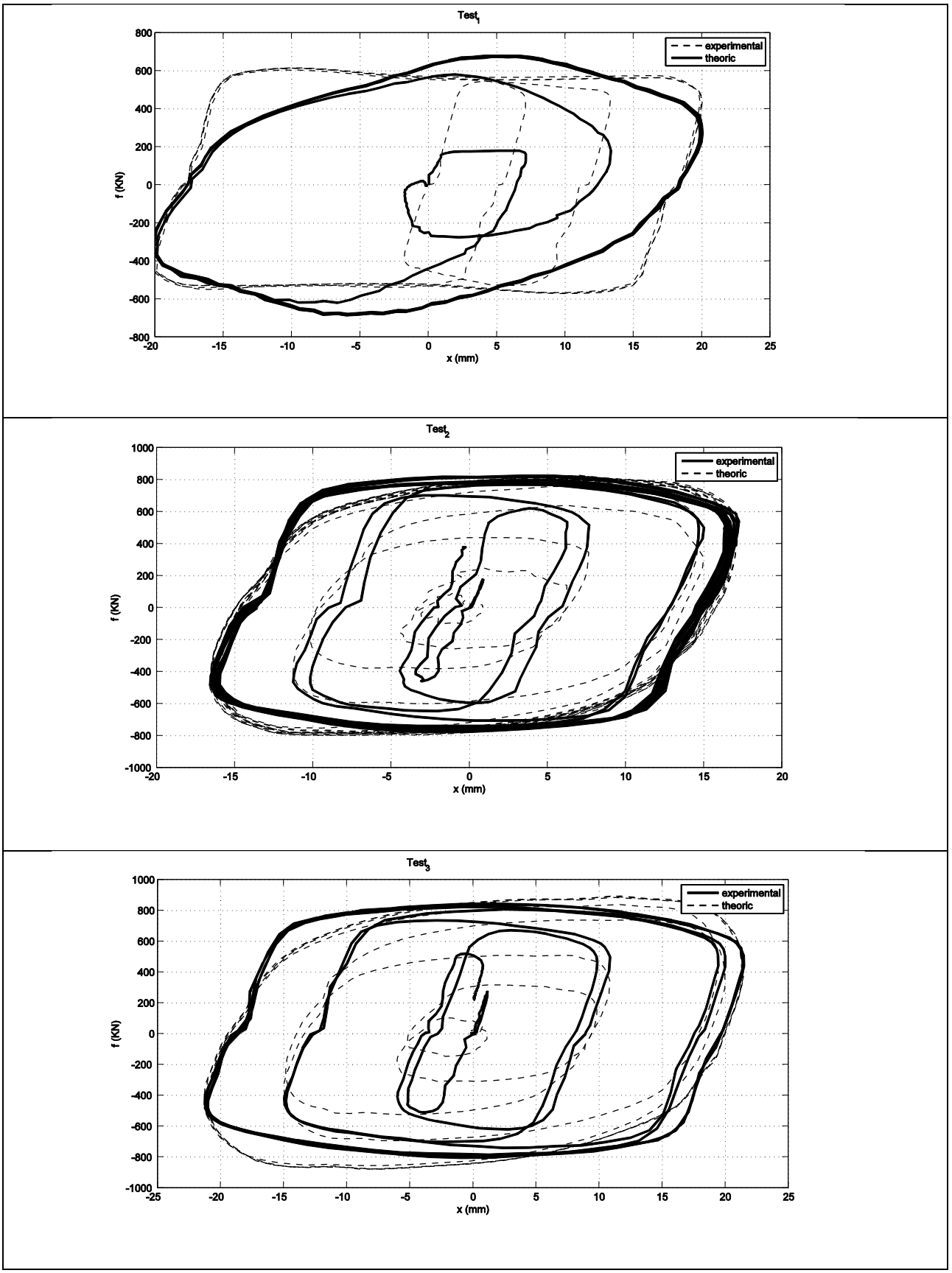

Figure 3 (a). Comparison between theoretical and experimental force -displacement relationships for the Voigt model.

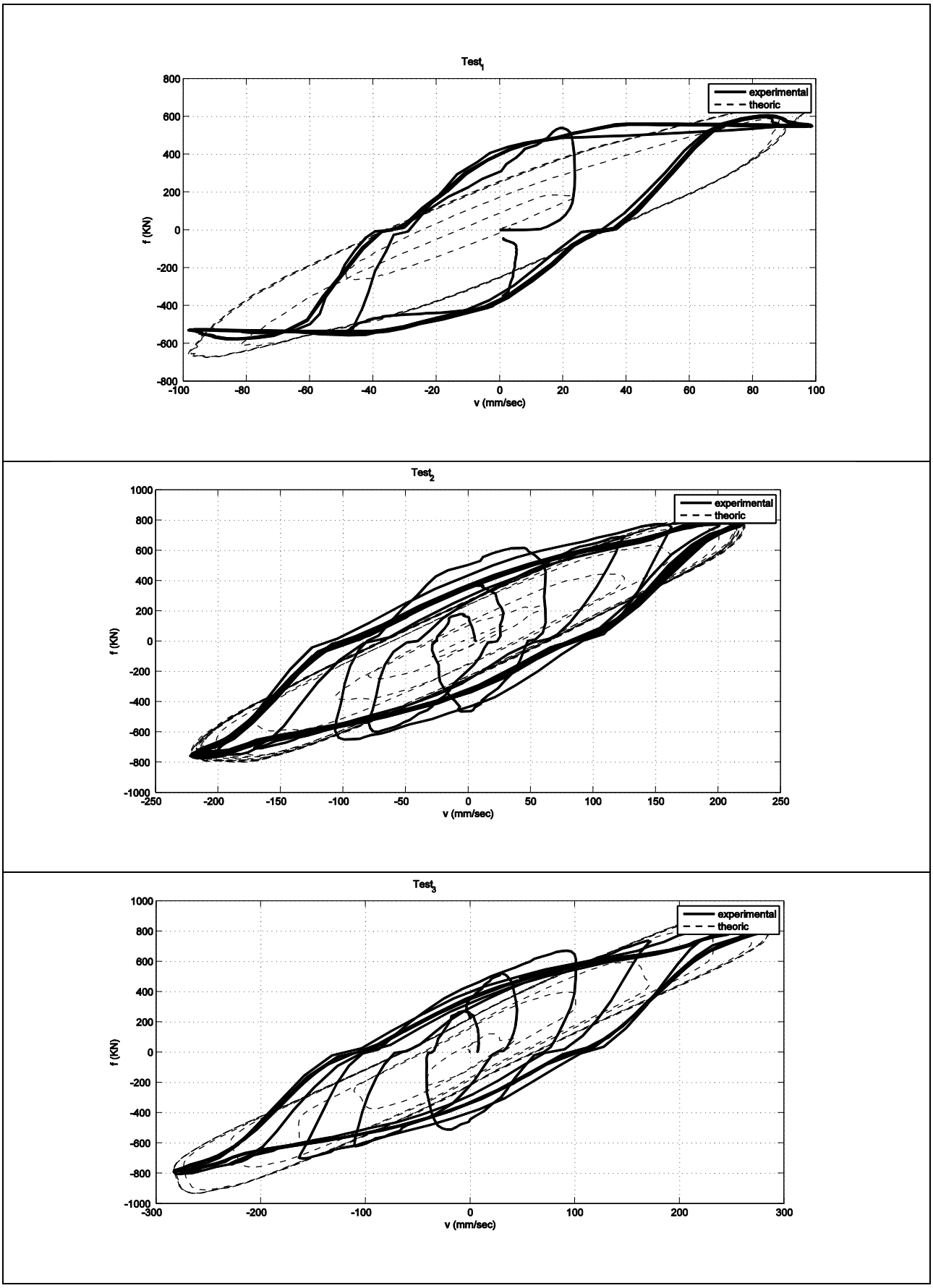

Figure 3 (b). Comparison between theoretical and experimental force – velocity relationships for the Voigt model.

It is evident that the classical Voigt model is unable to simulate the experimental loops because it shows approximately an elliptical shape which is rather dissimilar from the experimental loop recorded under different tests. This outcome is clearly manifest by numerical results of identification procedure (Table 3) which point out the higher value of the OF for the Voigt model. On the contrary, both the numerical results in Table 3 and hysteresis loops in Figure 5 point out that the generalized Maxwell model fits very well with the experimental loops under all the performed tests. However, also the capability of generalized Maxwell model to match the recorded hysteresis loops varies with the frequency and with the number of cycles; the greater performance (minimum of the OF) corresponds to test 2, i.e. when the frequency and the number of cycles increases. In effect, as previous mentioned, one can observe in each experimental test in Figures 3-6 that there is a transient phase in which, except for the generalized Maxwell model (Figure 6), the theoretical loops is unable to match with the experimental one and only after some cycles the theoretical loop fits the experimental one. This means that if the transient phase is large with respect to the entire duration of the load, a lower performance corresponds (greater OF) because this latter is computed over the entire duration. This consideration explains the increase of fitting as the number of cycles grows up (from test 3 to test 2) and this behavior can be noticed for all the analyzed models. This consideration can be appreciated in Figures 7 and 8, where for the four models the relationship force - displacement is plotted.

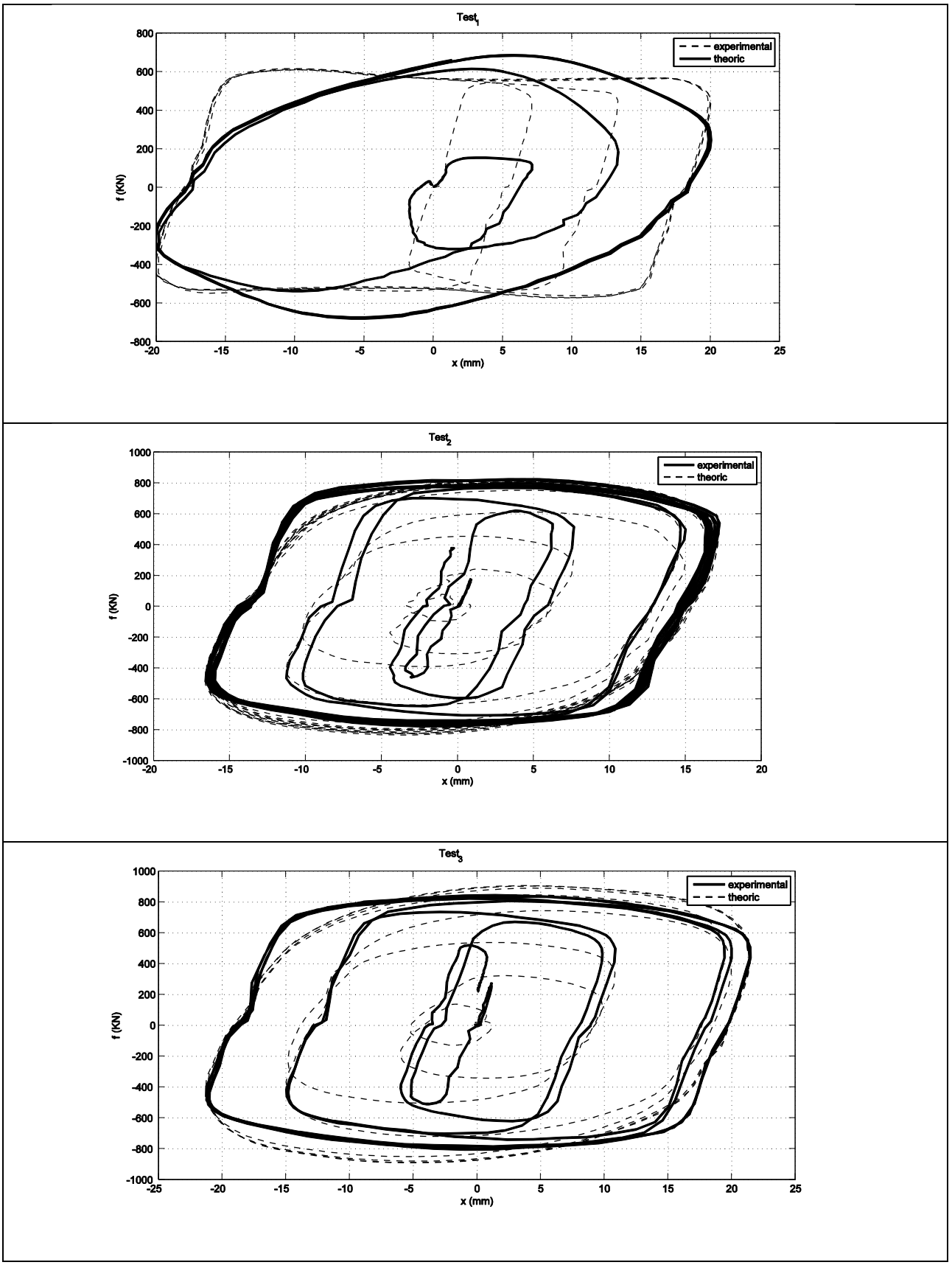

Figure 4 (a). Comparison between theoretical and experimental force -displacement relationships for the Maxwell model.

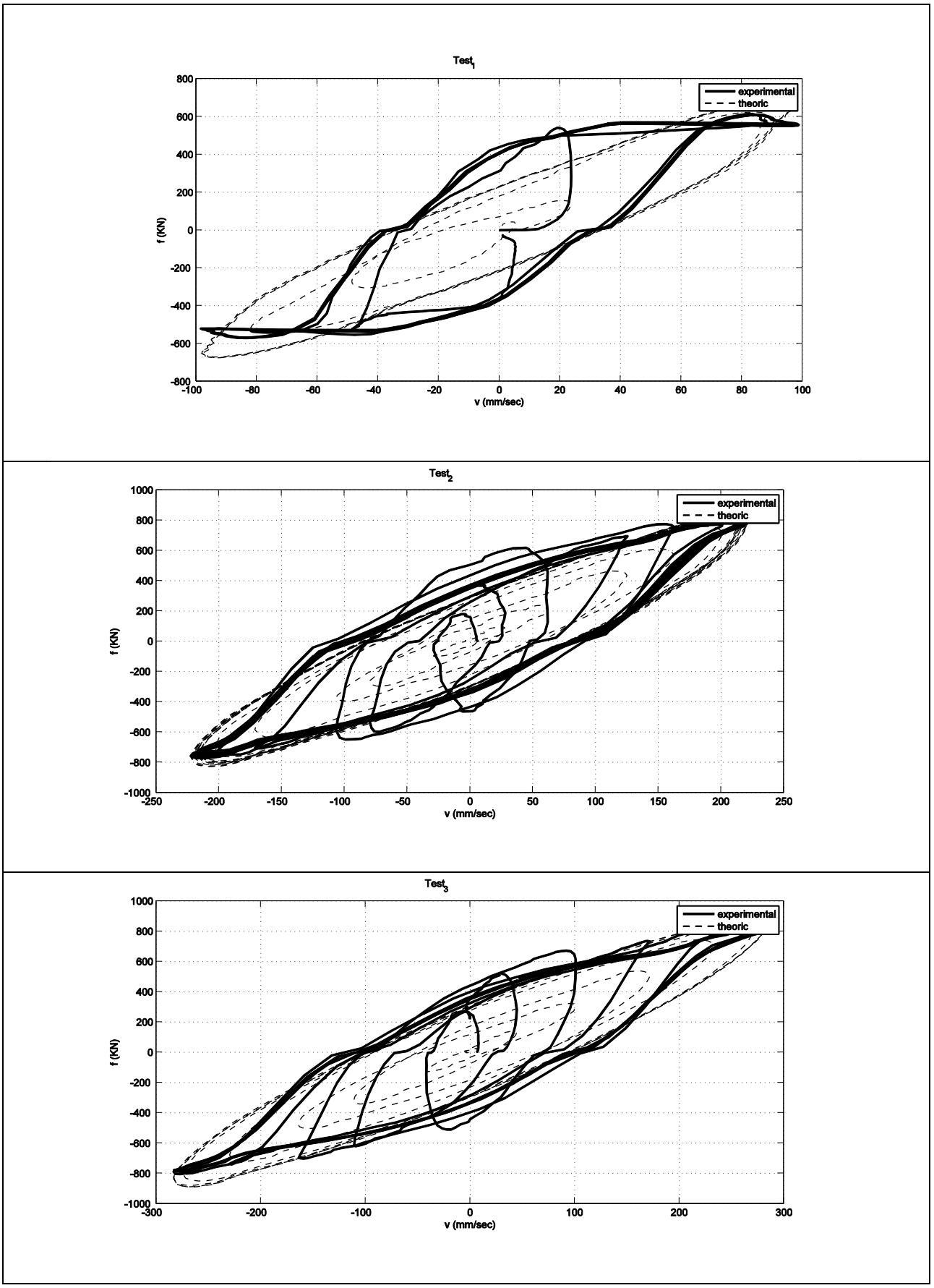

Figure 4 (b). Comparison between theoretical and experimental force -velocity relationships for the Maxwell model.

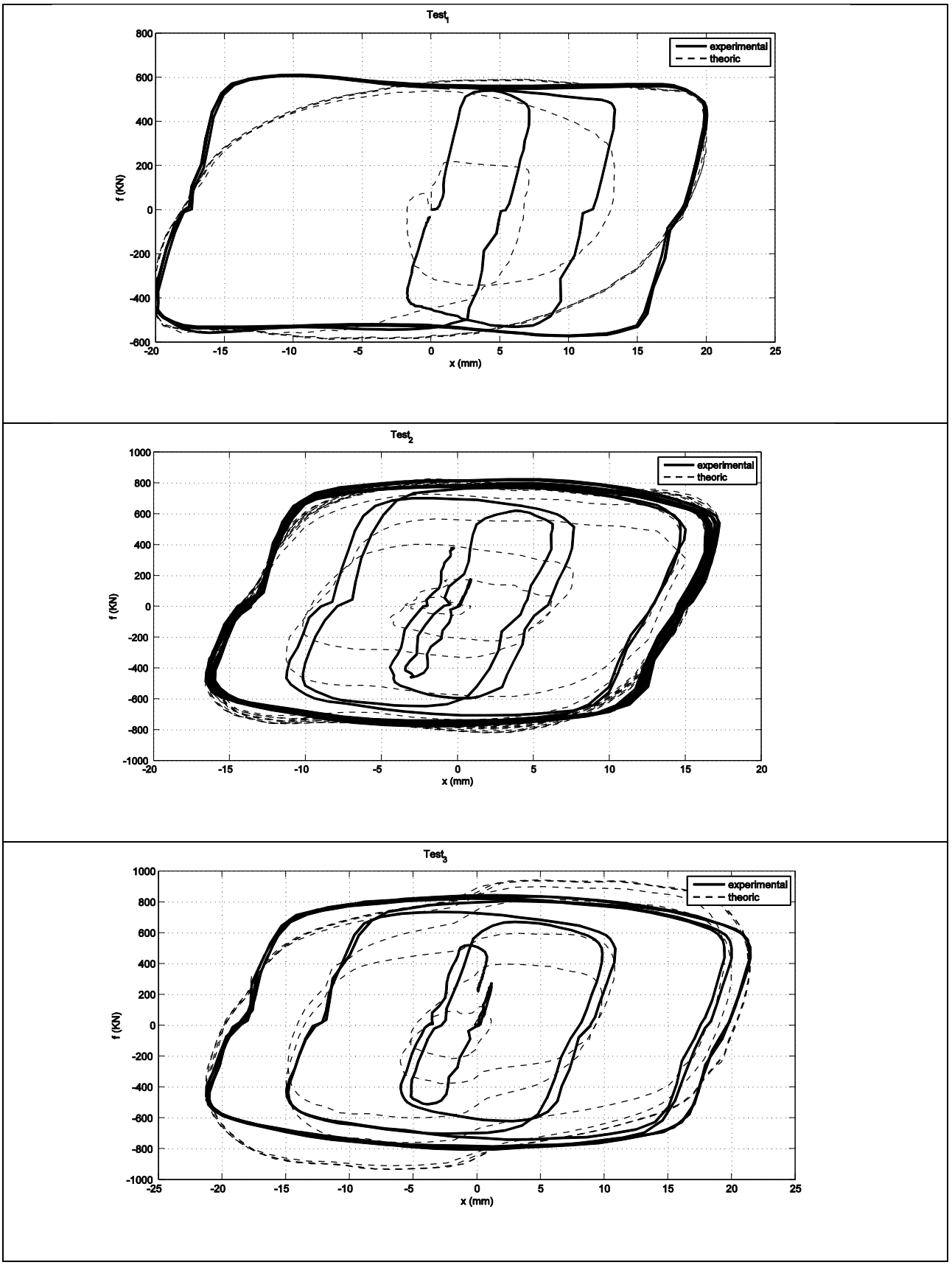

Figure 5 (a). Comparison between theoretical and experimental force -displacement relationships for the Generalized Voigt model.

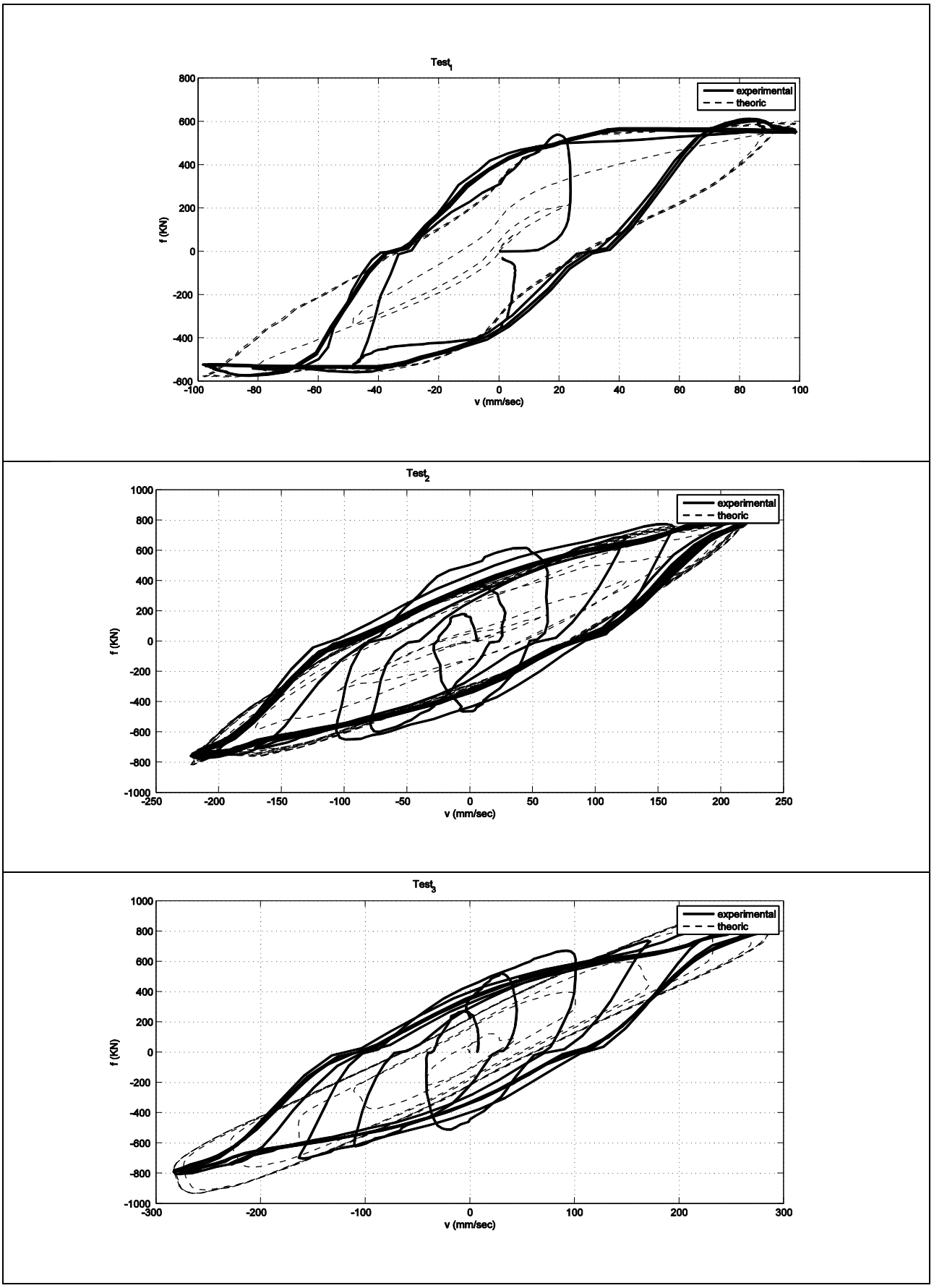

Figure 5 (b). Comparison between theoretical and experimental force –velocity relationships for the Generalized Voigt model.

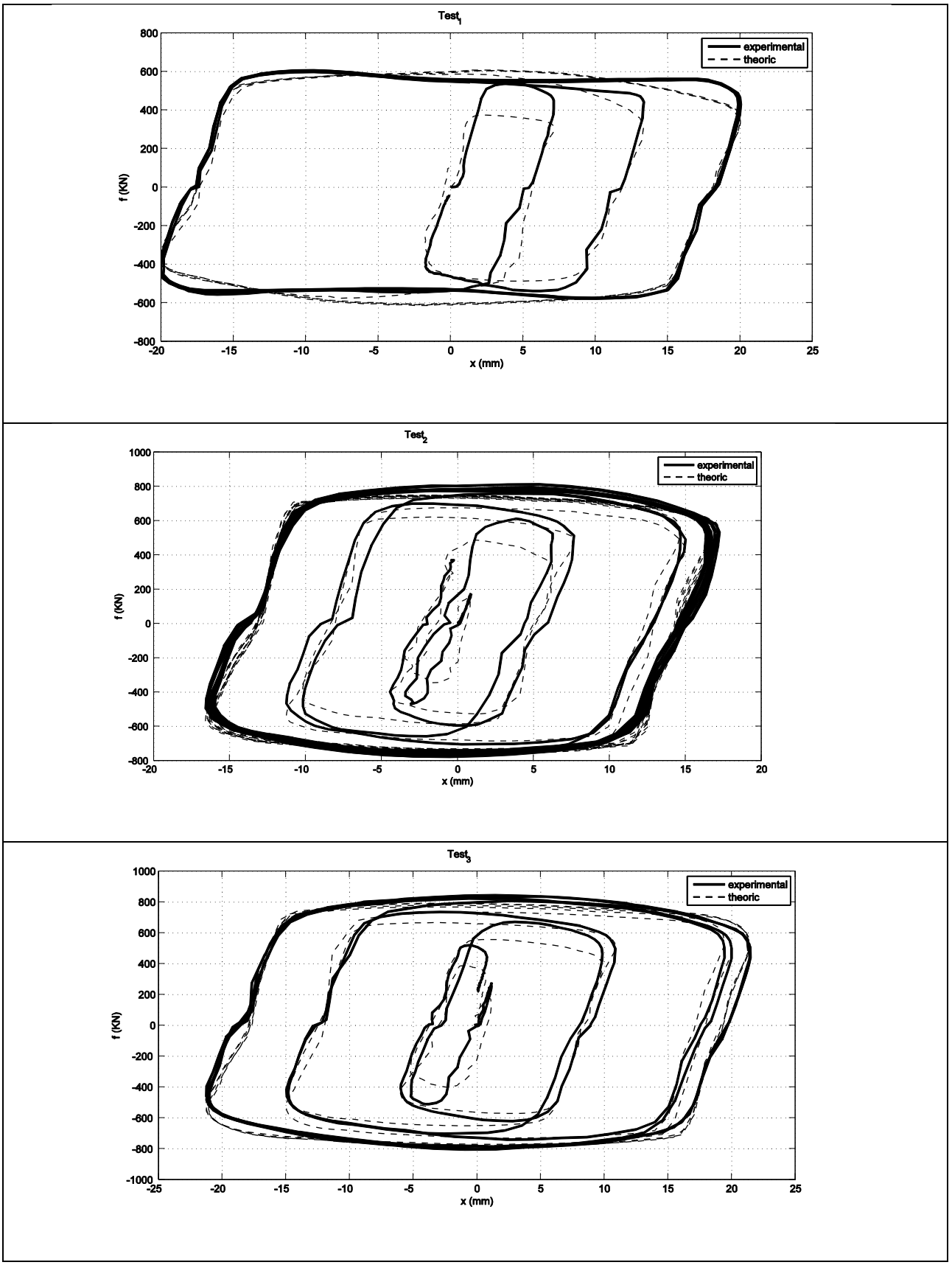

Figure 6 (a). Comparison between theoretical and experimental force -displacement relationships for the generalized Maxwell model.

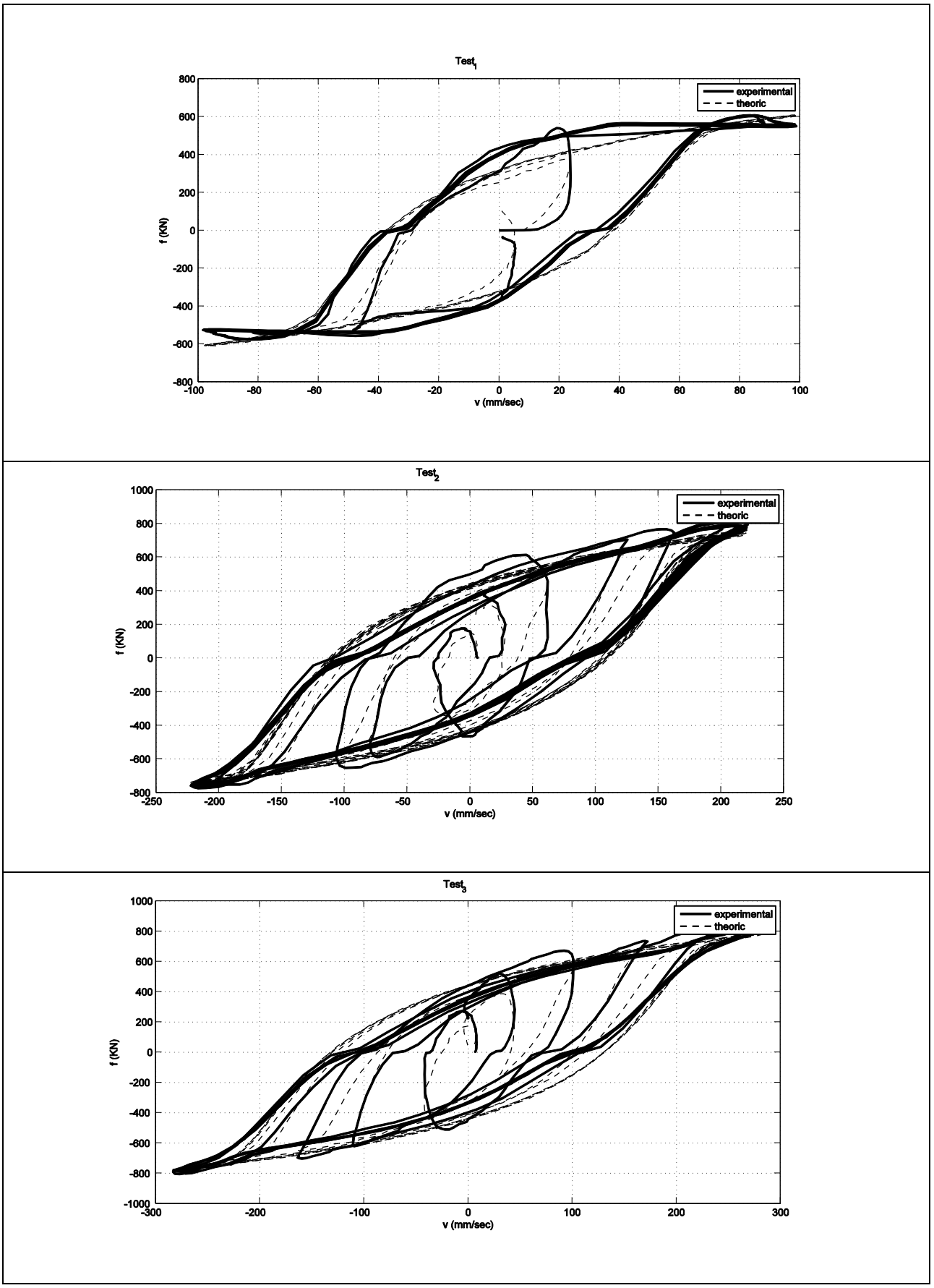

Figure 6 (b). Comparison between theoretical and experimental force -Velocity relationships for the generalized Maxwell model.

In addition, one can observe that from test 1 to test 3 (with higher frequency with respect to test 1), the matching of the generalized Maxwell model (but also the others) is inferior. The matching increases with the number of cycles, i.e. in the test 3, in which reaches the better performance for the reason previous explained. Also the standard Maxwell model works well in the test 2, whereas for low frequency the discrepancy between the standard and the generalized Maxwell model increases.

In the test 1 the Maxwell and Voigt models show approximately the same performance (OF=0.28). One should securely deduce that, concerning the variability of the matching with the frequency and the duration of the test, the model which works better is the generalized Maxwell model and that which works less is the Voigt one. This latter underestimates the force for all tests and especially under low frequency. **(v)** This justifies the use of series models with respect to parallel ones, that should be derived also from some mechanical considerations. Actually FVD presents an orifice that induces not only a turbulent oil flow during its activation, but also a quite high difference of pressure between the two damper oil tanks, and compressed oil shows an elastic behavior in this phase. Due to this, the force transmitted should be more reasonably represented by a series model instead that by a parallel one, as experimental results show. In addition to this, the Voigt model doesn't improve mostly in the passage to the non linear generalization, and one can observe only a little increase of the matching in the generalized Voigt model with respect to the standard one. The generalization of the model on the contrary produces a large improvement of the matching in the Maxwell model.

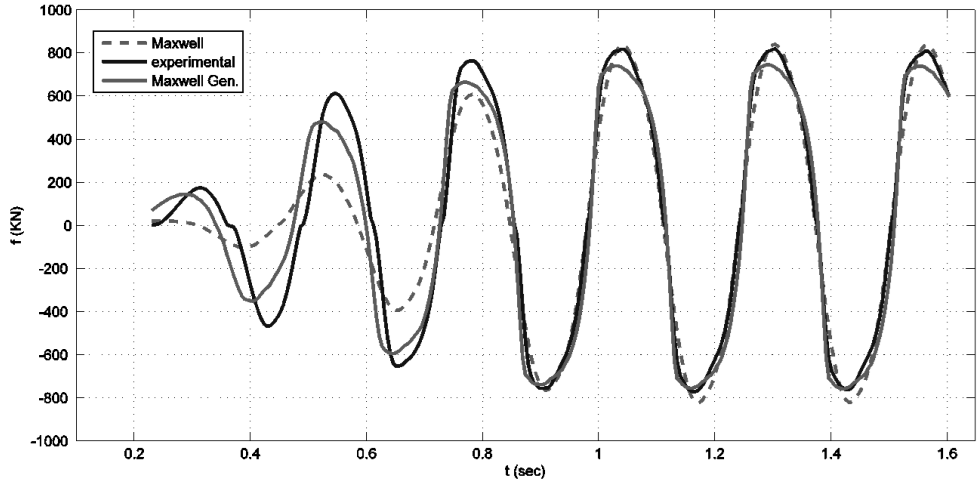

Figure 7. Comparison between theoretical and experimental force-time relationships for the Maxwell and Generalized Maxwell models.

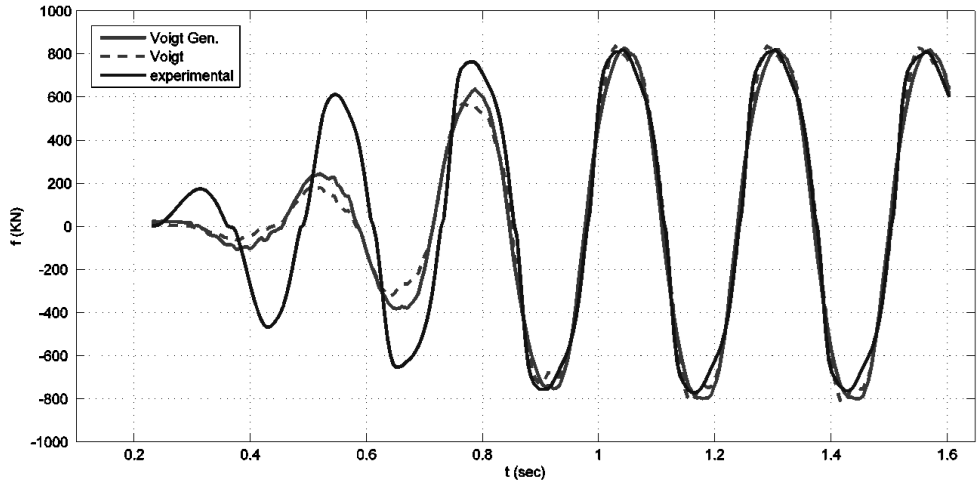

Figure 8. Comparison between theoretical and experimental force-time relationships for the Voigt and Generalized Voigt models.

Another important aspect that one should consider is the stability of identified parameters with respect to the test performed. In effect, also from this point of view, the Generalized Maxwell model performs very well with respect to the other ones, showing high stability with respect to the

test specimen. This aspect of the problem is very important in practical applications if one considers that when a FVD is installed on a structure it will be subject to diverse load conditions and, therefore, a suitable model should be stable when conditions such as load frequency and duration change. On the contrary, the model which shows the lower stability of identified parameters with respect to the test specimen is the Generalized Voigt one.

Moreover, in figures 3-6 also the relationship force-velocity is given. One should observe that the Generalized Maxwell model fits well also the force-velocity experimental loop, especially for high excitation frequency. However, also the standard Maxwell model is able to capture the experimental force -velocity loop, except for the test 1 The other models have a lesser ability to well represent real force - velocity loops.

There is also another important aspect to consider in this identification procedure; it uses an integral Objective Function, that simply means it minimizes differences between predicted and experimental device forces during the entire experiment. It takes into account not only stationary response (when sinusoidal displacement is reached) but also transient phase, at the beginning and at the end. This is strongly different from a standard frequency approach, that considers only stationary part. Moreover, in the proposed approach the transient phase contribution to the identification is function of its duration with reference to the entire experiment one. Some considerations should be added by observing, separately, the experimental-identified differences during the initial phase, when the imposed displacement grows up till to the request sinusoidal amplitude. In figures 7 and 8 differences between optimal parallel and series models (standard and generalized) with experimental behavior are reported.

It is evident that, in general, the Voigt model (fig. 8) doesn’t match well the transient phase, showing a good agreement with experimental data only when the stationary regime is reached. With more details, at the beginning, in the very first instants, both two Voigt models (standard and generalized) show a completely different phase with experimental data. Moreover, the generalized

model don’t increase significantly the accuracy. Differently, the Maxwell model shows a more accurate agreement with experimental data in this transient phase, and the generalized one exhibits a more accurate prediction instead of linear one. This should be an important point for the identification of such devices, because sinusoidal stationary experiments are quite far from real seismic excitations, where transient phase are dominant. With regard to this point it seems that standard Maxwell model presents the best agreement with experimental data not only during stationary but also during non stationary excitation, and so it will be used also for this reason.

6. Numerical study on a single degree of freedom system equipped with FVD

In the previous section it has been concluded that the generalized Maxwell model is able to accurately capture the hysteretic behavior of fluid viscous damper under harmonic excitation, demonstrating at the same time a great stability of identified parameters under various test conditions. In this section, in order to further investigate the effectiveness of the generalized Maxwell model, a sequence of simulations are performed to evaluate the seismic response of a single degree of freedom system, which simply models a structural system vibrating in its fundamental motion, under a real earthquake ground motion and equipped with a FVD. The earthquake motion selected is the El Centro record (comp. S00E) of the 1940 Imperial Valley earthquake. The selected system has mass m= 1000 kg, a damping coefficient equal to 2% and a natural period of 0.5 sec.

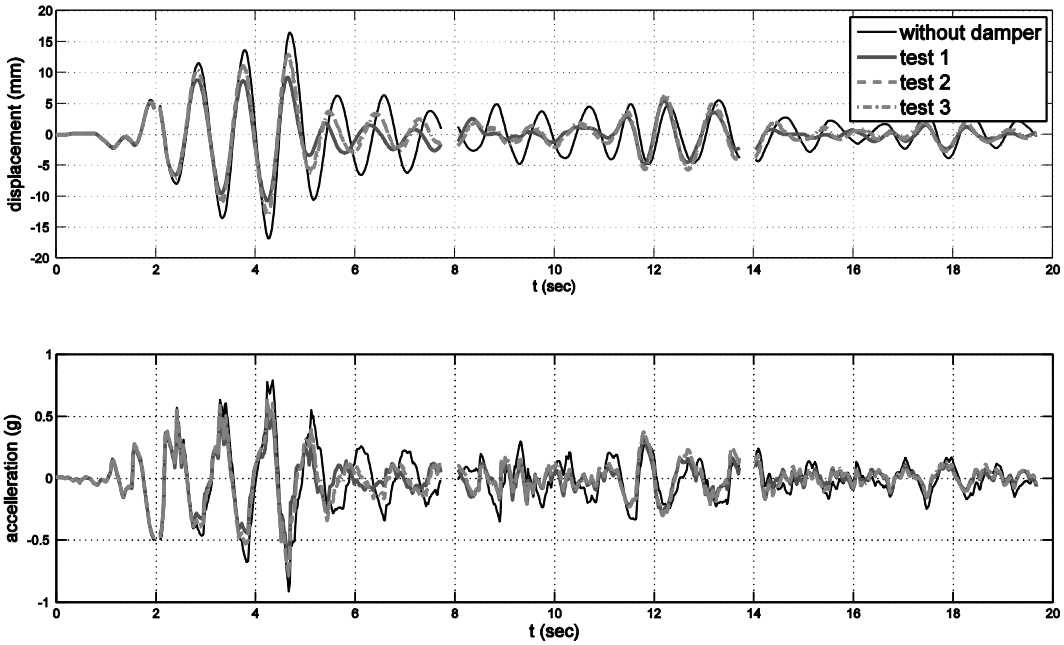

Figure 9. Comparison between displacement and acceleration time histories for a single DOF system without damper, and equipped with FVD. The Voigt model has been utilized, whose parameters have been identified under the three tests.

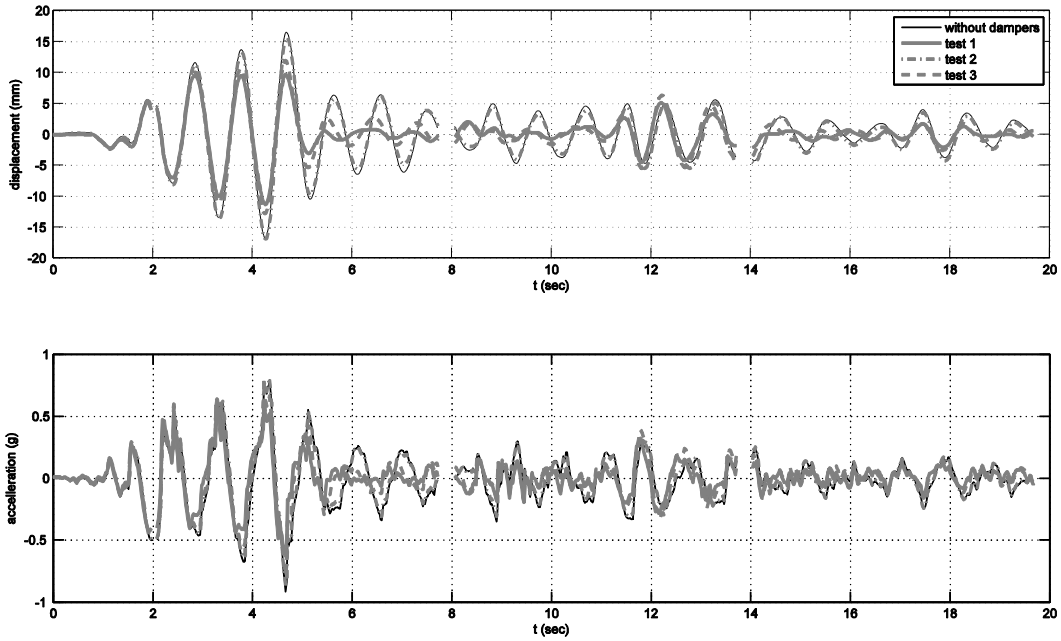

Figure 10. Comparison between displacement and acceleration time histories for a single DOF system without damper, and equipped with FVD. The Generalized Voigt model has been utilized, whose parameters have been identified under the three tests.

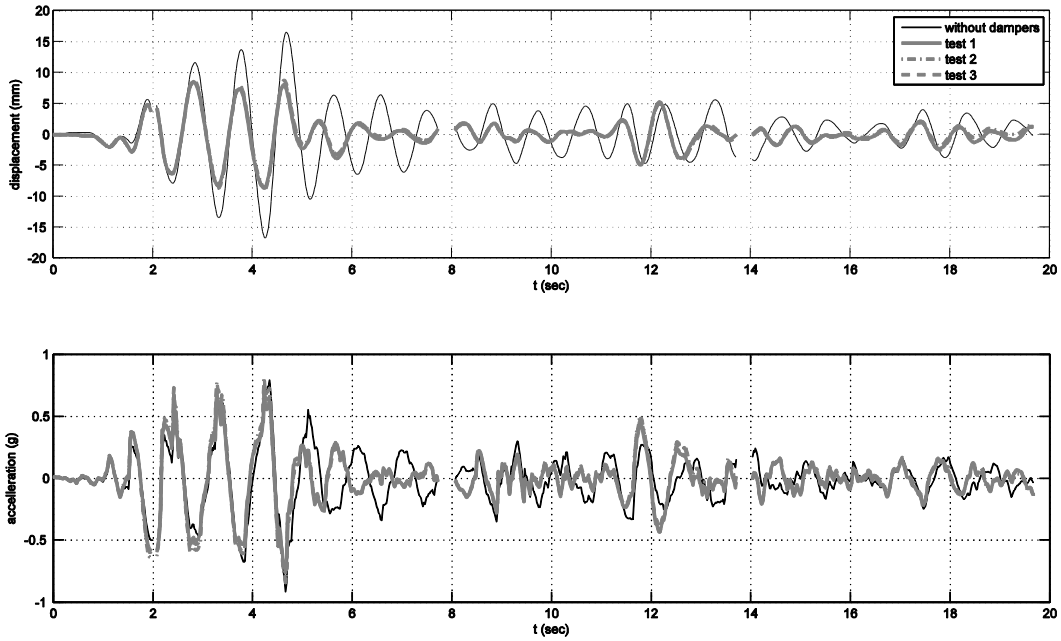

Figure 11. Comparison between displacement and acceleration time histories for a single DOF system without damper, and equipped with FVD. The Maxwell model has been utilized whose parameters have been identified under the three tests.

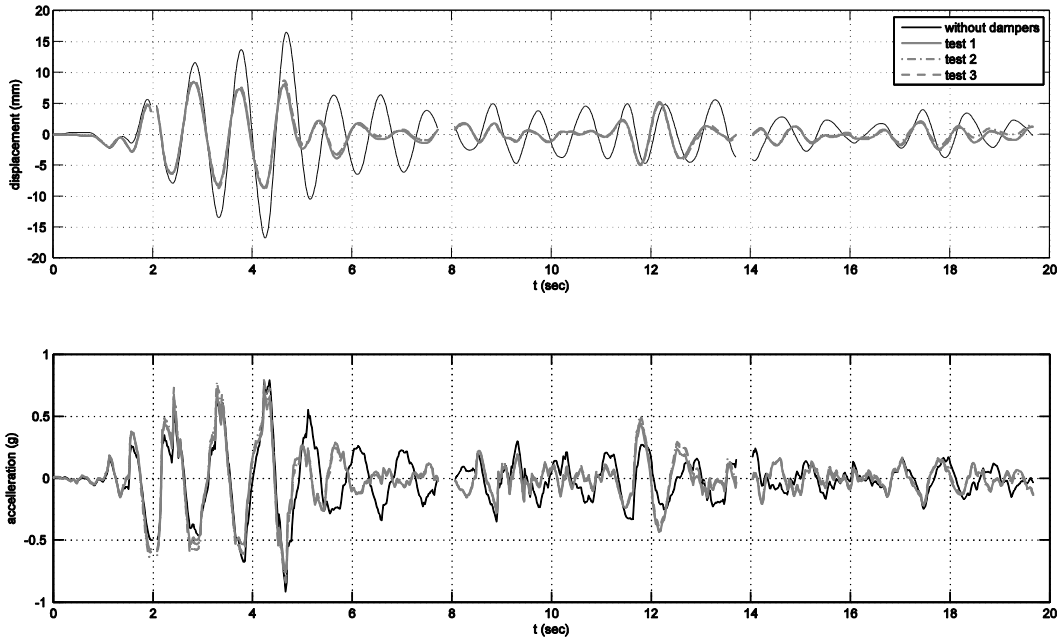

Figure 12. Comparison between displacement and acceleration time histories for a single DOF system without damper, and equipped with FVD. The Generalized Maxwell model has been utilized whose parameters have been identified under the three tests.

Under the El Centro Earthquake, Figures 9-12 compare the displacement and acceleration time histories of the SDOF system without protection and equipped with FVD. In each figure, corresponding to the four analyzed models, four different responses are plotted which correspond to three set parameters obtained under the three test conditions and to the system without FVD.

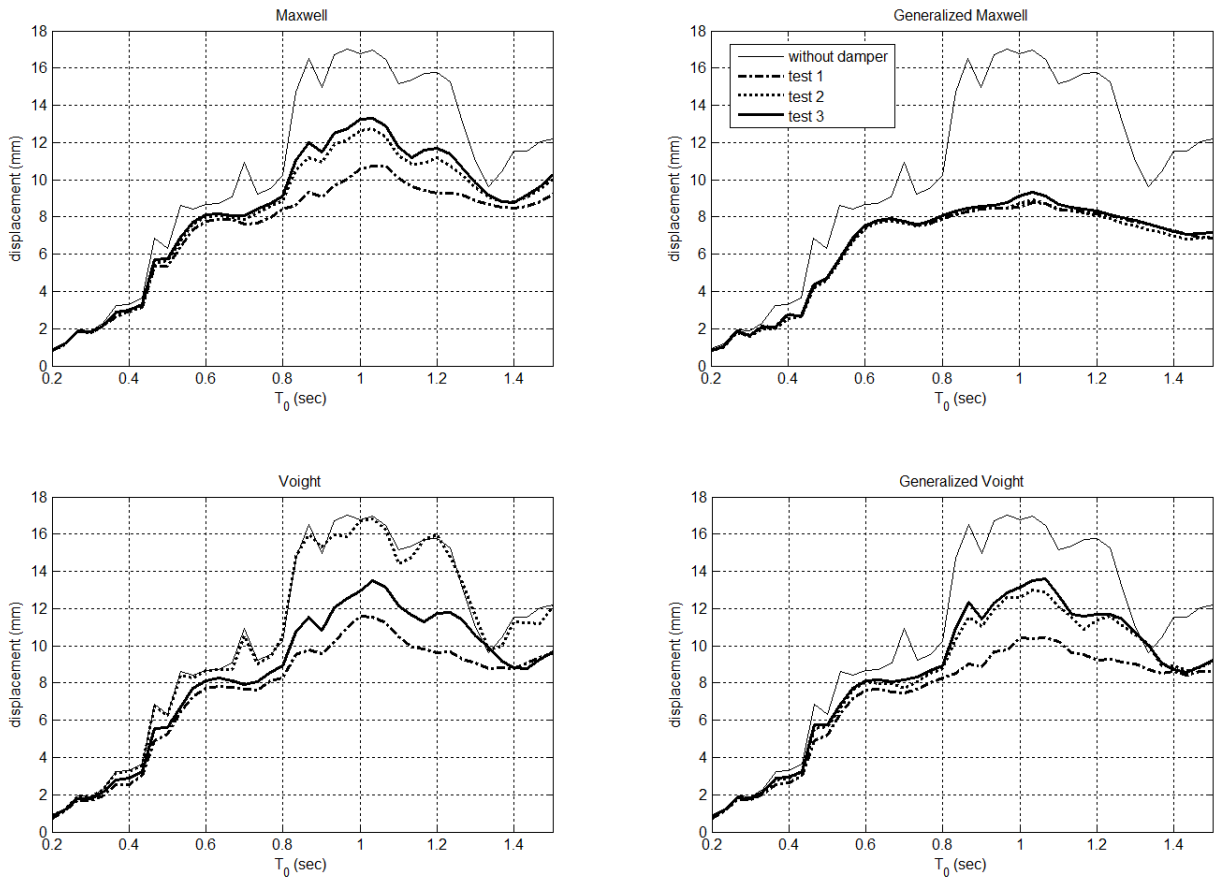

Figure 13. Comparison between spectral response for a single DOF system, without damper and equipped with FVD. For each model the parameters identified under the three tests have been utilized.

A first observation that can be carried out is that the modeling of FVD can affect the real evaluation of damper efficiency in reducing dynamic response of the main system. In effect, the different models adopted in this study, from the simple linear to the more comprehensive non-linear ones, can differently capture the real behavior of FVD . In effect, if a simple linear model is adopted, this can underestimate the FVD performance with respect to the generalized models. This last, taking properly into account the real dissipative capacity of FVD, produces a larger evaluation of the reduction of the response of the main system with respect of the reduction evaluated by adopting a linear model, such as the Voigt one (Figure 9). For this last model, in addition the

evaluation of the response reduction is affected by the parameters which have been evaluated under different test conditions. If the FVD is modeled by means of the generalized Kelvin-Voigt model (Figure 10) a larger evaluation of the response reduction is attained, observing at the same time a reduced variability with respect the test specimen from which the parameters have been identified..

If the Maxwell model (Figure 11) is selected to model the FVD, the evaluation of the main system response reduction is larger with respect to the same evaluation attained by adopting standard and generalized Kelvin-Voigt models. This obvious depends on the different ability of the models to capture the real FVD behavior. Figure 12 shows, finally, that the adoption of the Generalized Maxwell gives the higher reduction of the structural response under El Centro Earthquake.

Figure 13 shows the spectral response obtained considering the four analyzed models under the El Centro earthquake. Also if these results concern only a single seismic records and must not be generalized, some considerations should be done. The remarks above carried out are better noticeable in the spectral response, where the great superiority of the Generalized Maxwell model is clear in capturing the real behavior of FVD, showing at the same time a very good stability of identified parameters. Therefore, one should conclude that the Generalized Maxwell model is very suitable to model the real behavior of FVD. Another important aspect that one should consider is the stability of identified parameters with respect to the test performed. In effect, also from this point of view the Generalized Maxwell model performs very well with respect to the other ones, showing high stability with respect to the test specimen. It is clear, however, that these conclusions are in particular correct for this specific earthquake, and therefore they should be considered as an indicative result that will be deeply analyzed in the future.

7. Conclusions

This paper focuses on the generalized Kelvin-Voigt and Maxwell models for FVD; the resistant forces of both spring and dashpot elements in these two generalized models have fractional exponential coefficients. In order to assess the efficiency of these generalized models to capture the hysteretic behavior of real FVD, analytical models have been tested experimentally; identification scheme is developed comparing the experimental and the analytical values of the forces experienced by the device under investigation, where the experimental one has been recorded during the dynamic test while the analytical one is obtained by applying the time history of displacements to the candidate mechanical law. The parametric identification of a real fluid viscous damper has been developed by Particle Swarm Optimization (PSO).

The results have shown that the generalized Maxwell model fits very well with experimental test for all test conditions; on the contrary, the model which works poorer is the Voigt one. This latter underestimates the force for all tests and especially under low frequency.

Also numerical simulation under real seismic event shows the superiority of the Generalized Maxwell model, both in capturing the real behavior of FVD and in stability with respect to the test conditions from which parameters have been assessed.

REFERENCES

Aprile A, Inaudi JA and Kelly JM (1997) Evolutionary model of viscoelastic dampers for structural applications. Journal of Engineering Mechanics 123:551–60.

Atanackovic TM (2002) A modified Zener model of a viscoelastic body. Continuum Mechanics Thermo Dynamics 14:137–48.

Galucio AC, Deu JF and Ohayon R (2004) Finite element formulation of viscoelastic sandwich beams using fractional derivative operators. Computational Mechanics 33:282–91.

Gaul L, Schmidt A (2002) Parameter identification and FE implementation of a viscoelastic constitutive equation using fractional derivatives. PAMM (Proc Appl Math Mech) 1(1):153–4.

Gerlach S, Matzenmiller A (2005) Comparison of numerical methods for identification of viscoelastic line spectra from static test data. International Journal of Numerical Methods in Engineering 63:428–54.

Hansen S 2007 Estimation of the relaxation spectrum from dynamic experiments using Bayesian analysis and a new regularization constraint. Rheological Acta 47:169–78.

Hatada T, Kobori T, Ishida M and Niwa N (2000) Dynamic analysis of structures with Maxwell model. Earthquake Engineering and Structural Dynamics 29:159–76.

Jiu-Hong J, Hong-Xing H and Xiao-Yao S (2007) Viscoelastic Behavior Analysis and Application of the Fractional Derivative Maxwell Model

Journal of Vibration and Control. 13: 385-401,

Kennedy J, Eberhart R (1995) Particle Swarm Optimization. Proceedings of IEEE International Conference on Neural Networks IV: 1942–1948.

Lee SH, Son DI, Kim J and Min KW (2004) Optimal design of viscoelastic dampers using eigenvalue assignment. Earthquake Engineering and Structural Dynamics 33: 521-542.

Makris N, Constantinou MC (1991) Fractional-derivative Maxwell model for viscous dampers. Journal of Structural Engineering 117:2708–24.

Marano GC, Trentadue F and Greco R (2007) Stochastic optimum design criterion for linear damper devices for seismic protection of buildings. Structural and Multidisciplinary Optimization 33(6): 441-455.

Marano GC, Greco R and Sgobba S (2010) A comparison between different robust optimum design approaches: application to tuned mass dampers. Probabilistic Engineering Mechanics 25: 108-118.

Papoulia KD, Panoskaltsis VP, Korovajchuk I and Kurup NV (2010) Rheological representation of fractional derivative models in linear viscoelasticity. Rheological Acta 49(4): 381-400.

Park SW (2001a) Analytical modeling of viscoelastic dampers for structural and vibration control. International Journal of Solids and Structures 38:8065–92.

Park SW (2001b) Rheological Modeling of Viscoelastic Passive Dampers. Smart Structures and Materials: Damping and Isolation, SPIE 2001 4331: 343-354.

Pritz T (1996) Analysis of four-parameter fractional derivative model of real solid materials. Journal of Sound and Vibration 195(1):103–15.

Schmidt A, Gaul L (2002) Finite element formulation of viscoelastic constitutive equations using fractional time derivatives. Journal of Nonlinear Dynamics 29:37–55.

Shukla AK, Datta TK (1999) Optimal use of viscoelastic dampers in building frames for seismic force. Journal of Structural Enginerring 125:401–9.

Singh MP, Moreschi LM (2002) Optimal placement of dampers for passive response control. Earthquake Engineering and Structural Dynamics 31:955–76.

Singh MP, Verma NP and Moreschi LM (2003) Seismic analysis and design with Maxwell dampers. Journal of Engineering Mechanics 129:273-282.

Soong TT and Dargush GF (1998). Passive energy dissipation systems in structural engineering. John Wiley & Sons.

Soong TT, Spencer BF (2002) Supplemental energy dissipation: state-of-the-art and state-of-thepractice. Journal of Engineering Structures 24: 243–259.

Song DY, Jiang TQ (1998) Study on the constitutive equation with fractional derivative for the viscoelastic fluids – modified Jeffreys model and its application. Rheological Acta 37(5):512–7.

Syed Mustapha SMFD, Philips TN (2000) A dynamic nonlinear regression method for the determination of the discrete relaxation spectrum. Journal of Physics D; 33:1219–29.

Yun HB, Tasbighoo F, Masri SF, Caffrey JP, Wolfe RW, Makris N. and Black N (2008) Comparison of Modeling Approaches for Full-scale Nonlinear ViscousDampers, Journal of Vibration and Control 14(1-2): 51-76.

Yun CB, Bahng, EY (2000) Substructural identification using neural networks. Computers and Structures **77**: 41-52.

Zhao-Dong X (2007) Earthquake Mitigation Study on Viscoelastic Dampers for Reinforced Concrete Structures, Journal of Vibration and Control 13 (1): 29–43.

Zhao-Dong Xu, Deng-Xiang Wang and Chun-Fang Shi (2011)) Model, tests and application design for viscoelastic dampers. Journal of Vibration and Control. 17(9): 1359-1370.